frontiers in Cellular Neuroscience

METHODS
published: 24 July 2019
doi: 10.3389/fncel.2019.00312

Dedicated Setup for the Photoconversion of Fluorescent Dyes for Functional Electron Microscopy

Katharine L. Dobson[1,2], *Carmel L. Howe*[3], *Yuri Nishimura*[1,4] *and Vincenzo Marra*[1]*

[1] Department of Neuroscience, Psychology and Behaviour, University of Leicester, Leicester, United Kingdom, [2] Centre for Discovery Brain Sciences, University of Edinburgh, Edinburgh, United Kingdom, [3] Department of Bioengineering, Imperial College London, London, United Kingdom, [4] Sussex Neuroscience, School of Life Sciences, University of Sussex, Brighton, United Kingdom

Here, we describe a cost-effective setup for targeted photoconversion of fluorescent signals into electron dense ones. This approach has offered invaluable insights in the morphology and function of fine neuronal structures. The technique relies on the localized oxidation of diaminobenzidine (DAB) mediated by excited fluorophores. This paper includes a detailed description of how to build a simple photoconversion setup that can increase reliability and throughput of this well-established technique. The system described here, is particularly well-suited for thick neuronal tissue, where light penetration and oxygen diffusion may be limiting DAB oxidation. To demonstrate the system, we use Correlative Light and Electron Microscopy (CLEM) to visualize functionally-labeled individual synaptic vesicles released onto an identified layer 5 neuron in an acute cortical slice. The setup significantly simplifies the photoconversion workflow, increasing the depth of photoillumination, improving the targeting of the region of interest and reducing the time required to process each individual sample. We have tested this setup extensively for the photoconversion of FM 1-43FX and Lucifer Yellow both excited at 473 nm. In principle, the system can be adapted to any dye or nanoparticle able to oxidize DAB when excited by a specific wavelength of light.

Keywords: FM1-43, Lucifer Yellow, synaptic vesicle (SV), functional labeling, electron microscopy, CLEM, correlative light electron microscopy, synapse

OPEN ACCESS

Edited by:
Federico F. Trigo,
Université Paris Descartes, France

Reviewed by:
Céline Auger,
UMR8118 Physiologie Cérébrale, France
Jorge E. Moreira,
University of São Paulo, Brazil

***Correspondence:**
Vincenzo Marra
vm120@le.ac.uk

Specialty section:
This article was submitted to Cellular Neurophysiology, a section of the journal Frontiers in Cellular Neuroscience

Received: *30 April 2019*
Accepted: *25 June 2019*
Published: *24 July 2019*

Citation:
Dobson KL, Howe CL, Nishimura Y and Marra V (2019) Dedicated Setup for the Photoconversion of Fluorescent Dyes for Functional Electron Microscopy. Front. Cell. Neurosci. 13:312. doi: 10.3389/fncel.2019.00312

1. INTRODUCTION

The study of presynaptic organization requires the analysis of both functional and structural aspects of axons and their synaptic compartments (for a review see Debanne et al., 2011). While, for structurally well-characterized synapses, vesicular release can be studied using mainly electrophysiological methods (Jonas et al., 1993; Neher and Sakaba, 2001; Pulido et al., 2015), the study of central synapses often requires a combination of imaging methods. A number of super-resolution techniques can provide information on the morphology of labeled structures with nanometer accuracy (see Gramlich and Klyachko, 2019), however, Electron Microscopy (EM) is still the only imaging technique able to provide contextual information at the ultrastructural level. Classic EM cannot provide any functional information and, to overcome this limitation, a number of Correlative Light and Electron Microscopy (CLEM) techniques have been developed over the years to study live tissue (Maranto, 1982; Harata et al., 2001; Darcy et al., 2006; Ratnayaka et al., 2011; Shu et al., 2011; Peddie et al., 2017; de Beer et al., 2018). Many CLEM techniques rely on

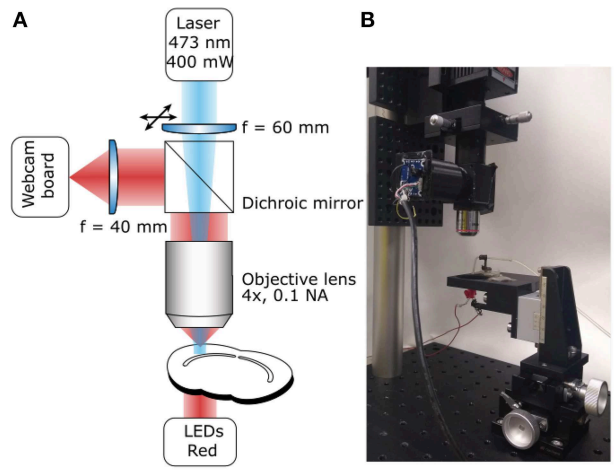

FIGURE 1 | Photoconversion Rig. **(A)** Diagram of the light path for both sample illumination (blue) and visualization (red). **(B)** Photograph of a working setup including sample illumination and visualization paths and sample holder.

the conversion of the fluorescent signal into an electron dense one and when this process requires light activation it is generally referred to as photoconversion. For over 30 years, photoconversion of diaminobenzidine (DAB) has been used to observe, at the ultrastructural level, functionally identified neurons (Maranto, 1982; Smith and Bolam, 1990; Viney et al., 2013). Harata et al. (2001) have shown for the first time that FM1-43 photoillumination in fixed cell cultures can be used to precipitate DAB into an osmiophilic polymer selectively in synaptic vesicles that underwent release and endocytosis in the presence of the dye. In spite of its usefulness, DAB photoconversion in thick neuronal tissue has only been employed by a relatively small number of research groups. A number of different protocols have been published to describe the technique in a range of different preparations and using different modes of light delivery to drive the photoconversion (Opazo and Rizzoli, 2010; Marra et al., 2014; Sabeva and Bykhovskaia, 2017).

Here, we present a low-cost system to drive targeted photoconversion of DAB in thick neuronal tissue. The intent of this article is not to describe the entire photoconversion procedure [already presented by Marra et al. (2014)], but to provide instructions to build a photoconversion setup to easily identify and illuminate a region of interest in a controlled manner.

2. EQUIPMENT

The photoconversion setup (**Figure 1**) consists of a high-power excitation light laser, an optical microscope for monitoring the sample during photoconversion and a simple stage to hold the sample and supply the oxygen required for DAB polymerization. We have included a list of the components (**Table 1**) required to build the system described here but we have not included general laboratory supplies.

2.1. Excitation Light Path

The system's main purpose is to deliver high-power excitation light over a large volume of tissue. The wavelength of the excitation light will depend on the fluorophore used. The system described here is built to photoconvert FM 1-43FX and Lucifer Yellow (excitation peaks at 473 and 425 nm, respectively), for this reason we chose a 473 nm Diode-Pumped Solid State (DPSS) laser as the light source, however, high-power (>300 mW) single-wavelength LEDs would also work. The light path is extremely simple to minimize attenuation (**Figure 1A**), it consists of a lens focussing the laser beam on the back focal aperture of a 4X air objective. Underfilling the objective aperture produces an approximately collimated beam providing a larger volume of evenly photoilluminated tissue compared with what would be achieved overfilling the objective aperture. The light will still be scattered by the tissue but the illuminated region will be effectively thicker driving the reaction over a larger volume for the same exposure time compared to previously reported results (Marra et al., 2014). Photoconverted vesicles can be observed at 85 µm below the slice surface, a 35 µm improvement over the previous method (Marra et al., 2012, ; data not shown). Between the focussing lens and the objective, the light goes through a 505 nm short-pass dichroic mirror. While the dichroic mirror attenuates the laser intensity, it also allows simultaneous visualization of the sample and of the photoilluminated area for precise positioning. This system ensures that over 20% of the laser output reaches the focal plane of the objective with an homogeneously illuminated area of 0.65 mm ^{2}. The fine position of the illuminated area can be adjusted using an XY lens translator. This component is not strictly required, however, it allows fine adjustments improving accuracy and reducing the chance for experimenters' error. Given the large volume illuminated, the power density is comparable to the previously reported one (Marra et al., 2014) and unlikely to directly damage fixed tissue. However, non-specific DAB oxidation may lead to precipitates that could obscure or damage the region of interest. The easiest solution to this issue, is to perform live labeling at least 20 µm below the surface of the tissue, when possible.

2.2. Sample Visualization Path

A critical step, in the photoconversion procedure, is the identification of the region of interest. In this photoconversion system, the objective used to deliver the excitation light is also used to image the sample which is illuminated from below with dim throughhole red LEDs. The red LEDs' light is unlikely to excite and photobleach the fluorophores and can be used to monitor the progress of the photoconversion reaction. The red light illuminating the sample will reach the objective, be reflected by the dichroic mirror and imaged using a simple webcam (**Figure 1**). We found that a large field of view is useful to identify the region of interest, particularly in acute brain slices. Such large field of view can be obtained by using a camera with a large sensor (e.g., >1/1.8") or by reducing the objective's magnification. Here, we have used an inexpensive webcam with a small sensor 1/4", removed the casing and glued it to a 3D-printed adaptor (**Figure 2A**). The lens creating the image on the webcam sensor is placed at only 70 mm from the objective's back aperture,

TABLE 1 | List of components.

Component	Supplier	Product code	Notes
EXCITATION LIGHT PATH			
473 nm Laser	Eksma Optics	DPSS-473-H	This could be replaced with any appropriate high-power light source. Single wavelength Macro LEDs are a viable alternative.
Main post	Thorlabs	P50/M	The 50 cm post is the main body of the setup. A shorter version (30 cm–P30/M) would be appropriate if space is a concern.
Post mounting clamps	Thorlabs	C1545/M	Two are required one to mount the laser, one for the cube holding the dichroic mirror.
Spacers	Thorlabs	BA2S8/M	Two are required to mount the laser so that its output is aligned with the rest of the optics.
Steel post L=50.8 mm	Edmund Optics	83–133	This post is needed to mount the cube holding the dichroic mirror on the mounting clamps. The additional 0.8 mm length compared with the Thorlabs equivalent allowed for a better match with the laser output but may not be required for other systems.
Planconvex lens f= 60 mm	Edmund Optics	47–347	This lens focusses the laser beam on the back focal plane of the objective.
XY lens translator	Thorlabs	ST1XY-S/M	To move the lens used to focus the laser
Lens tube spacer	Thorlabs	SM1S10	To connect the XY lens translator with the cube.
Dichroic mirror cube	Thorlabs	CM1-DCH/M	The rest of the optical components will be connected to this cube.
Short-pass dichroic mirror	Laser2000	FF505-SDi01	This 25 x 36 mm mirror will let over 90% of the laser light through while reflecting the transmitted light to the webcam.
SM1 to RMS thread adapter	Thorlabs	SM1A3TS	Allows the objective to be mounted directly on the mirror holding cube.
4X Objective	Thorlabs	RMS4X	Objective used for light delivery and sample imaging.
SAMPLE VISUALIZATION PATH			
Lens tube for focussing lens	Thorlabs	SM1L25	This tube connects to the cube and holds the lens focussing the image on the camera sensor.
Bi convex lens f= 40 mm	Thorlabs	LB1027	This is used to image on the webcam sensor.
3D printed webcam adapter	3D printed		See SCAD file.
Webcam			Any standard webcam would work but its original lens will need to be removed.
STAGE AND OXYGEN DELIVERY			
XYZ Stage	Laser2000	TAR-38405L-M6	3-axis translator for sample positioning.
Stage	3D printed		See SCAD file.
Capillary holder	3D printed		See SCAD file.
Petri dish insert	3D printed		See SCAD file.
Glass O-ring	Glass blowing workshop		Normally cut from a 19mm capillary.

providing an effective magnification of 1.5X. This provides an adequate compromise between magnification and field of view. The ability to identify the region of interest with a large field of view greatly speeds up the positioning process down to a few minutes. Depending on user's experience and region of interest's size, the positioning process can take up to 45 min when using a high power objective and following a "roadmap" acquired before tissue fixation, particularly without the aid of fluorescence.

2.3. Stage and Oxygen Delivery

To minimize the cost, a stage was designed using OpenSCAD (openscad.org) and 3D-printed using an Ultimaker2$^+$ 3D-printer. The stage is connected to the 3-axis translator and used to hold and position the sample. Magnetic metal should be glued on the stage to position a capillary holder (**Figure 2C**). The stage includes a support for the throughhole LEDs used to illuminate the sample (**Figures 1B**, **2B**). Once ready for photoconversion, the fixed tissue is placed in a 35 mm petri dish containing a plastic insert (**Figure 2C**) and held down with a glass O-ring (19 mm O.D.) with nylon strings (Marra et al., 2014). Once the user has identified the region of interest, PBS can be replaced with the DAB solution and oxygenated using Carbogen (95% O_2 and 5% CO_2). Carbogen is delivered using a glass capillary with an opening of $>150\,\mu m$. The capillary is held by a 3D-printed holder (**Figure 2C**) with a magnet glued to its base for positioning. The plastic insert has two functions: keeping the sample and the O-ring in the center of the petri dish and avoiding bubbles from floating over the sample and thus scattering the light (**Figure 2C**).

3. MATERIALS AND METHODS

3.1. Brain Slice Preparation

This study was conducted in accordance with the UK Animals (Scientific Procedures) Act, 1986 and following institutional regulations by the University of Leicester, animals were sacrificed under Schedule 1 and the project did not require full review and approval by the Home Office. Experiments were performed

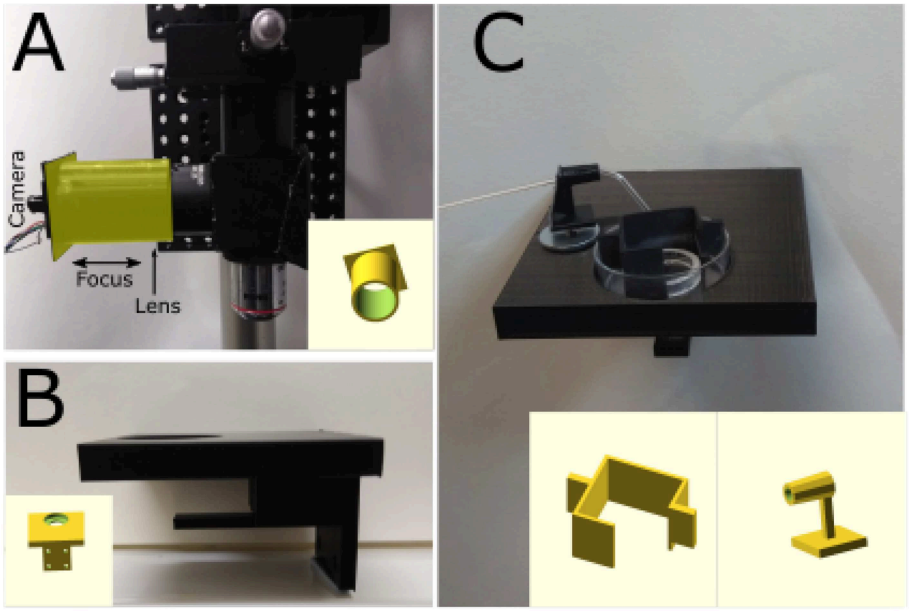

FIGURE 2 | 3D-printed components. **(A)** Photograph of a simple adaptor (highlighted in the yellow) for mounting a webcam board onto a Thorlabs 1" lens tube. The lens focusing the image on the sensor is placed inside the tube and the 3D-printed adaptor can be moved to focus the image. Insert: 3D model of the adaptor. **(B)** Photograph of stage mounted on 3-axis translator. Metal disks were glued and covered with transparent plastic to avoid DAB-induced oxidation. Insert: 3D model of the stage. **(C)** Sample in a 35 mm petri dish held in position by a 19 mm glass ring with nylon string across its middle and plastic box that prevents sample movement and bubbles covering the sample.The sample would placed under the glass ring. Glass capillary holder with a magnet mounted at its bottom to hold it in position. The capillary is used to oxygenate the solution and facilitate DAB photoconversion. Insert: 3D model of petri dish box and capillary holder.

in CBA/Ca mice of either sex postnatal day 15—20. Animals were humanely killed by cervical dislocation and cessation of circulation was confirmed by severing the carotid artery. The brain was rapidly removed and placed into ice-cold oxygenated artificial cerebrospinal fluid (aCSF) consisting of (in mM): 125 NaCl, 2.5 KCl, 26 $NaHCO_3$, 1.25 NaH_2PO_4, 25 glucose, 1 $MgCl_2$, 2 $CaCl_2$; pH 7.3 when bubbled with 95% O_2 and 5% CO_2. Auditory cortex slices were cut at a thickness of 350 µm using a vibrating microtome (Leica VT1200S) at an angle of 15° off horizontal to preserve thalamocortical projections (Llano et al., 2014). Slices were allowed to recover for 20 min at 32°C before being cooled to room temperature.

3.2. Electrophysiology and Cell Labeling

Whole-cell recordings were made from visually identified layer 5 pyramidal neurons. Intracellular recording solution consisted of (in mM): 115 $KMeSO_4$, 5 KCl, 10 HEPES, 10 creatine phosphate, 0.5 EGTA, 2 MgATP, 2 Na_2ATP, 0.3 Na_2GTP, 290 mOsm, with the addition of Lucifer Yellow (1 mg/mL, Sigma-Aldrich, ex/em 425/540 nm). After 5 min in whole-cell configuration a Z-stack image of the dye-loaded cell was acquired for later reference. A glass stimulating electrode filled with FM 1-43FX (20 µM in aCSF) (Thermofisher) was positioned ∼ 150 µm from the recorded cell soma at a depth equal to that of the recording electrode. Prior to the onset of dye application the stimulus intensity was set to give a reliable excitatory post-synaptic current (EPSC) amplitude of ∼200 pA, to ensure the recruitment of a large number of presynaptic terminals.

3.3. Vesicle Labeling

FM 1-43FX (Thermofisher, ex/em 473/585 nm) dye was locally applied by providing 1.03 bars of positive pressure for a total of 5 min. Two minutes after the start of dye application presynaptic terminals were stimulated at 10 Hz for 60 s using a stimulus isolator (Digitimer). Dye application continued for further 2 min for a total of 5 min dye application and 10 min in whole-cell configuration. The recording electrode was then carefully withdrawn to reseal the recorded cell and minimize Lucifer Yellow leakage.

3.4. Fixation and Photoconversion

Fixation and photoconversion were performed ensuring the samples' exposure to light was kept to a minimum and following the protocol of Marra et al. (2014). Slices were carefully removed from the recording chamber and fixed in 6% glutaraldehyde/2% paraformaldehyde in PBS using microwave-assisted fixation. Samples were blocked in 100 mM glycine solution for 1 h, rinsed in 100 mM ammonium chloride for 1 min, then washed in PBS. The sample was then positioned on the photoconversion setup (**Figure 1B**) with a fine bore glass capillary immersed to allow continuous bubbling with Carbogen throughout. PBS was replaced with 1 mg/mL DAB solution prepared in oxygenated PBS and incubated in the dark for 10 min. This was replaced with fresh oxygenated DAB solution and the photoconversion reaction initiated using the 473nm DPSS laser (**Figure 1A**). Before starting the photoconversion reaction, the laser should be set to a low power setting and positioned on the region of interest

using the fine XY lens translator while the transmission LEDs are on, to obtain an unequivocal image of the photoilluminated region on the sample. Reactions were monitored every 5–10 min and terminated when a defined dark region was visible on the slice. Since a number of factors may affect the time required to obtain a successful photoconversion, we recommend monitoring

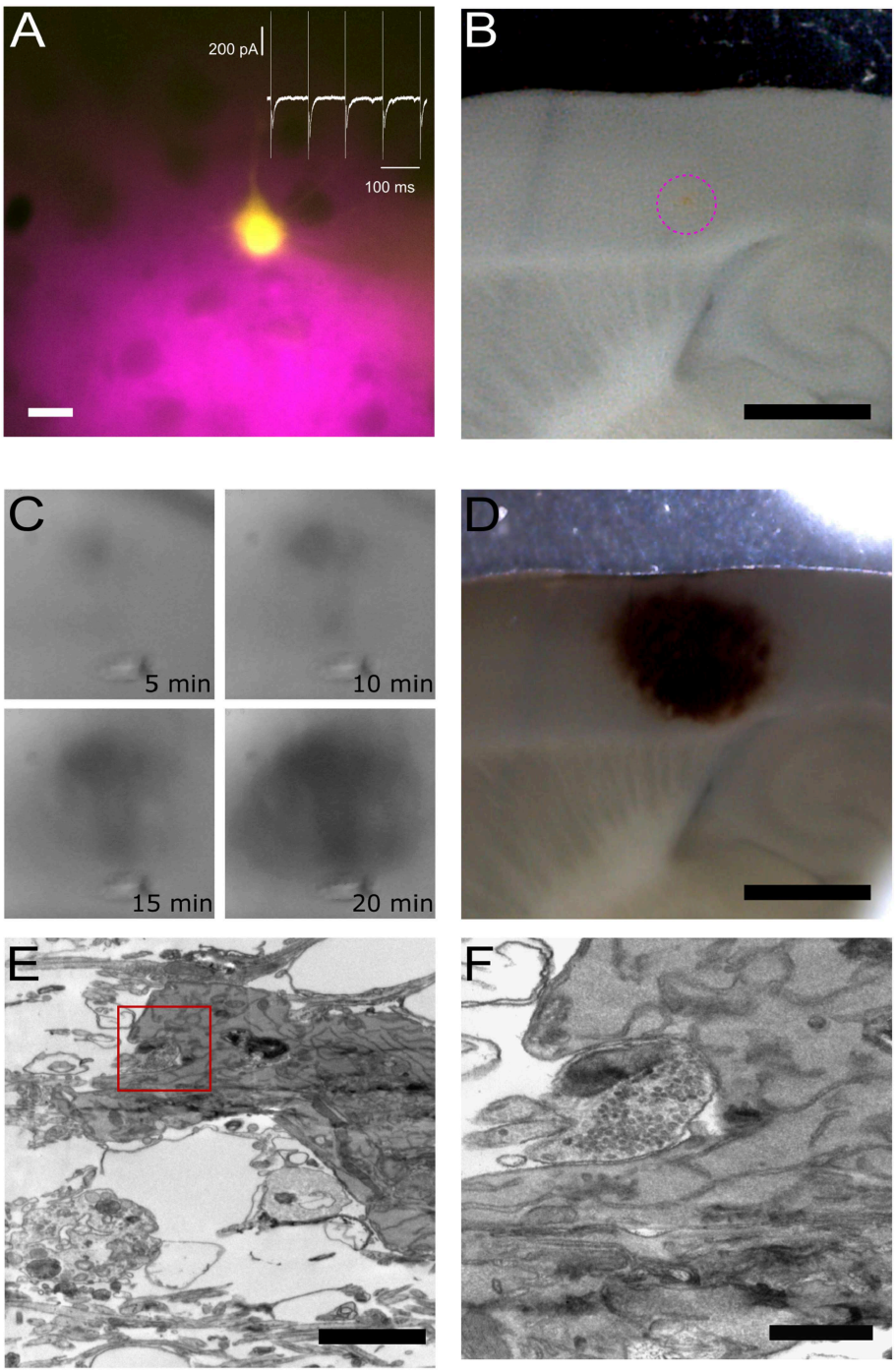

FIGURE 3 | Pre- and post-synaptic photoconversion anticipated results. **(A)** Pyramidal neuron loaded with Lucifer Yellow with region of pressure-applied FM dye highlighted in magenta. Insert: whole-cell voltage clamp recording from loaded cell. Scale bar: 20 μm. **(B)** Acute slice following fixation, with FM dye region clearly visible (magenta dashed circle). Scale bar: 1 mm. **(C)** Development of the photoconversion product monitored at 5 min intervals. **(D)** Photoconverted region extending across FM dye region and Lucifer Yellow-loaded neuron. Scale bar: 1 mm. **(E)** Electron micrograph of Lucifer Yellow-loaded neuron. Scale bar: 20 μm. **(F)** Higher magnification electron micrograph of the same spine as **(E)**, with FM-loaded vesicles observed in the presynaptic terminal. Scale bar: 500 nm.

the process at regular intervals (∼5 min) by powering down the laser and measuring the intensity of the transmitted light. In the first 10 min there should be a clear decrease in transmitted light intensity that will plateau when the photoconversion process is complete (see Marra et al., 2014). The photoconversion of FM-stained dead tissue will reduce light penetration as the reaction progresses. Using an approximately collimated beam ensures that a large volume is photoconverted before light penetration becomes an issue. The sample was then washed 3 x 5 min in PBS. An image of the photoconverted slice was captured and the sample trimmed for further processing.

3.5. Sample Processing for Electron Microscopy

Processing of the fixed photoconverted tissue for electron microscopy follows the protocol of Deerinck et al. (2010). Briefly, samples were washed with 0.15 M sodium cacodylate buffer prior to osmication (2% OsO_4, 1.5% $K4Fe(CN)_6$). Samples were then washed with dH_2O and incubated in 1% thiocarbohydrazide solution. Tissues were rinsed again in dH_2O and thereafter placed in 2% osmium tetroxide. Following this second exposure to osmium the tissues were washed with dH_2O then placed in 1% uranyl acetate at 4°C overnight. As an optional step, samples were then washed again with dH_2O and stained *en bloc* with freshly prepared 20 mM lead aspartate. After further dH_2O washes samples are serially dehydrated using a gradient of ethanol solutions and finally with 100% acetone. Samples were infiltrated with Durcupan^{TM} resin before being transferred to a BEEM capsule for embedding and polymerization. With reference to the image of the photoconverted tissue the sample was trimmed, ultrathin (∼70 nm) sections cut and mounted on copper grids. Sections were imaged on a JEOL 1400 transmission electron microscope equipped with an OptiMos (QImaging).

4. ANTICIPATED RESULTS

4.1. Simultaneous Photoconversion of FM 1-43FX and Lucifer Yellow

To show potential applications of the photoconversion setup, we have combined electrophysiological recordings of a neuron filled with Lucifer Yellow via a patch pipette with simultaneous loading of synaptic vesicles with FM 1-43FX. FM-loading is obtained by puffing the dye with a glass pipette which is also used to deliver the stimulation required for the labeling of synaptic vesicles (10 Hz, 60 s), vesicular release is monitored recording the post-synaptic neuron in voltage clamp (**Figure 3A**). Importantly, the choice of stimulation frequency and duration will depend on the biological question asked. For example, a 1 Hz stimulation for 30 s can be used to study single site release probability (Branco et al., 2010), stimulation frequencies of 10 Hz or above for 1 or 2 min may be used to label the entire recycling pool (Fornasiero et al., 2012) and higher frequency stimulations for few seconds may be used to label the readily releasable pool (Rey et al., 2015). The stimulation frequency used will also depend on the type of synapse probed. For example, at large release sites such as the Calyx of Held, a giant synapse in the auditory pathway, stimulations > 100 Hz are appropriate to recruit the total recycling pool (Lucas et al., 2018); similarly at neuromuscular junctions long high frequency stimulations (30 Hz, 5 min) may be needed (Denker et al., 2009).

Figure 3 provides an overview of typical results plus examples of the tissue at each stage of processing. The location of the two fluorophores, FM 1-43FX to label presynaptic vesicles and Lucifer Yellow to fill the post-synaptic cell, is visible throughout processing, thus giving the user confidence in the final structural information correlating with the functional readout from the electrophysiological assay. The site of delivery for FM 1-43FX can be easily visualized at low magnification (**Figure 3B**). Following fixation, the sample is moved to the photoconversion setup where the reaction's progression can be observed as a darkening of the tissue (Marra et al., 2014). Before processing for electron microscopy the photoconverted region appears as a dark spot on the tissue (**Figure 3D**). Electron dense structures are readily identifiable in the resultant electron micrograph as a soma containing DAB precipitate (**Figure 3E**) and photoconverted vesicles observed in the terminal opposite the labeled post-synaptic neuron (**Figure 3F**). Lucifer Yellow's absorption is only 25% at 473 nm and this appears sufficient to drive DAB photoconversion without excessive DAB-damage (**Figure 3E**).

Depending on the stimulation protocol, the approach demonstrated here can be used to investigate a number of key synaptic and cellular parameters, e.g., synaptic sites, release probability, recycling pool organization, and in general the impact of pre- and post-synaptic structures on synaptic function.

5. DISCUSSION

The functional study of axonal fine structures often requires a combination of fluorescence and electron microscopy. These measurements can be performed in parallel (Clayton et al., 2008; Cheung et al., 2010; Chung et al., 2010; Ratnayaka et al., 2012) or in a correlative way following the same axons and synapses from light to electron microscopy (reviewed by Branco and Staras, 2009; Begemann and Galic, 2016). In both cases, however, the measurements are limited to dissociated cell cultures. A number of new tools are being developed by commercial and academic research laboratories to simplify the CLEM workflow and to extend it to thick neuronal tissue. Some laboratories are developing new fluorescent proteins able to oxidize DAB in a light-independent way (Shu et al., 2011; Liss et al., 2015; de Beer et al., 2018), while others focus on new microscopes to improve the reliability of CLEM workflow (see Brama et al., 2016).

Here, we presented a simple setup to photoconvert fluorescent signals into electron dense ones. The setup is built to facilitate tracing of the region of interest in thick neuronal tissue improving CLEM workflows for *ex vivo* tissue. A dedicated setup can improve reliability and throughput of the photoconversion; these are the two main limiting factors in the diffusion of the technique. Compared with the use of a standard epifluorescence microscope, our setup increases the depth of photoillumination, improves the targeting of the region of interest and reduces the time required to process each individual sample. Commercial

epifluorescence microscopes have optics to ensure Köhler illumination of the sample, while offering a great advantage for imaging, such optics can attenuate a single wavelength light by ∼90% before it reaches a dichroic mirror and filter, which will further attenuate the light. Additionally, most photoillumination approaches for thick tissue require the "sacrifice" of a high power dipping objective to deliver light (Marra et al., 2014) as, once used for DAB photoconversion, a dipping objective should not be used for live tissue imaging. Additionally, air objectives will not be stained by repeated exposure to DAB, while dipping objectives, even with careful cleaning, will stain over time increasing the photoconversion time and affecting the quality of the image used for positioning.

The budget used for building the setup in 2016 was ∼4500€, with over 50% of the budget used to purchase the laser. However, a suitable 473 nm DPSS laser can now be found for much lower prices or substituted by high-power single-wavelength LEDs, lowering the cost of the entire system to ∼3000€, comparable with the cost of a dedicated high quality dipping objective for photoconversion of thick neuronal tissue (Marra et al., 2014). We demonstrate that the setup described can be used for the simultaneous photoconversion of FM 1-43FX and Lucifer Yellow, allowing the study of cellular ultrastructure and activity and release probability at individual release sites.

DATA AVAILABILITY

The datasets generated for this study are available on request to the corresponding author.

ETHICS STATEMENT

This study was carried out in accordance with the recommendations of Animals (Scientific Procedures) as amended in 2012.

AUTHOR CONTRIBUTIONS

KD acquired the data and tested the setup. YN tested the setup. CH assisted with the design of the setup. VM designed, built and tested the setup. All authors contributed to the manuscript.

FUNDING

The work was funded by the Wellcome Trust Seed Awards in Science 108201/Z/15/Z.

ACKNOWLEDGMENTS

The authors would like to thank the Core Bioscience Services for access to the experimental animals, the fluorescence microscope setup by Professor Nicholas Hartell and the electron microscope. In particular, we would like to thank Natalie Allcock for the assistance with the preparation of the samples for electron microscopy and the acquisition of the images. We would also like to thank Amy Richardson for building the PWM laser power regulator and Drs. James McCutcheon and Joern Steinert for lending us components to test the early configuration of the setup. A previous version version of this article was published as preprint on www.biorxiv.org (Dobson et al., 2019).

REFERENCES

Begemann, I., and Galic, M. (2016). Correlative light electron microscopy: connecting synaptic structure and function. *Front. Synapt. Neurosci.* 8:28. doi: 10.3389/fnsyn.2016.00028

Brama, E., Peddie, C. J., Wilkes, G., Gu, Y., Collinson, L. M., and Jones, M. L. (2016). ultralm and minilm: locator tools for smart tracking of fluorescent cells in correlative light and electron microscopy. *Wellcome open Res.* 1:26. doi: 10.12688/wellcomeopenres.10299.1

Branco, T., Marra, V., and Staras, K. (2010). Examining size-strength relationships at hippocampal synapses using an ultrastructural measurement of synaptic release probability. *J. Struct. Biol.* 172, 203–210. doi: 10.1016/j.jsb.2009.10.014

Branco, T., and Staras, K. (2009). The probability of neurotransmitter release: variability and feedback control at single synapses. *Nat. Rev. Neurosci.* 10, 373–383. doi: 10.1038/nrn2634

Cheung, G., Jupp, O. J., and Cousin, M. A. (2010). Activity-dependent bulk endocytosis and clathrin-dependent endocytosis replenish specific synaptic vesicle pools in central nerve terminals. *J. Neurosci.* 30, 8151–8161. doi: 10.1523/JNEUROSCI.0293-10.2010

Chung, C., Barylko, B., Leitz, J., Liu, X., and Kavalali, E. T. (2010). Acute dynamin inhibition dissects synaptic vesicle recycling pathways that drive spontaneous and evoked neurotransmission. *J. Neurosci.* 30, 1363–1376. doi: 10.1523/JNEUROSCI.3427-09.2010

Clayton, E. L., Evans, G. J., and Cousin, M. A. (2008). Bulk synaptic vesicle endocytosis is rapidly triggered during strong stimulation. *J. Neurosci.* 28, 6627–6632. doi: 10.1523/JNEUROSCI.1445-08.2008

Darcy, K. J., Staras, K., Collinson, L. M., and Goda, Y. (2006). Constitutive sharing of recycling synaptic vesicles between presynaptic boutons. *Nat. Neurosci.* 9, 315–321. doi: 10.1038/nn1640

de Beer, M. A., Kuipers, J., van Bergen En Henegouwen, P. M. P., and Giepmans, B. N. G. (2018). A small protein probe for correlated microscopy of endogenous proteins. *Histochem. Cell Biol.* 149, 261–268. doi: 10.1007/s00418-018-1632-6

Debanne, D., Campanac, E., Bialowas, A., Carlier, E., and Alcaraz, G. (2011). Axon physiology. *Physiol. Rev.* 91, 555–602. doi: 10.1152/physrev.00048.2009

Deerinck, T., Bushong, E., Lev-Ram, V., Shu, X., Tsien, R., and Ellisman, M. (2010). Enhancing serial block-face scanning electron microscopy to enable high resolution 3-d nanohistology of cells and tissues. *Microsc. Microanal.* 16, 1138–1139. doi: 10.1017/S1431927610055170

Denker, A., Kröhnert, K., and Rizzoli, S. O. (2009). Revisiting synaptic vesicle pool localization in the drosophila neuromuscular junction. *J. Physiol.* 587, 2919–2926. doi: 10.1113/jphysiol.2009.170985

Dobson, K. L., Howe, C. L., Nishimura, Y., and Marra, V. (2019). Dedicated setup for the photoconversion of fluorescent dyes for functional electron microscopy. *BioRxiv* [Preprint]. doi: 10.1101/622639

Fornasiero, E. F., Raimondi, A., Guarnieri, F. C., Orlando, M., Fesce, R., Benfenati, F., et al. (2012). Synapsins contribute to the dynamic spatial organization of synaptic vesicles in an activity-dependent manner. *J. Neurosci.* 32, 12214–12227. doi: 10.1523/JNEUROSCI.1554-12.2012

Gramlich, M. W., and Klyachko, V. A. (2019). Nanoscale organization of vesicle release at central synapses. *Trends Neurosci.* 42, 425–437. doi: 10.1016/j.tins.2019.03.001

Harata, N., Ryan, T. A., Smith, S. J., Buchanan, J., and Tsien, R. W. (2001). Visualizing recycling synaptic vesicles in hippocampal neurons by

fm 1-43 photoconversion. *Proc. Natl. Acad. Sci. U.S.A.* 98, 12748–12753. doi: 10.1073/pnas.171442798

Jonas, P., Major, G., and Sakmann, B. (1993). Quantal components of unitary epscs at the mossy fibre synapse on ca3 pyramidal cells of rat hippocampus. *J. Physiol.* 472, 615–663. doi: 10.1113/jphysiol.1993.sp019965

Liss, V., Barlag, B., Nietschke, M., and Hensel, M. (2015). Self-labelling enzymes as universal tags for fluorescence microscopy, super-resolution microscopy and electron microscopy. *Sci. Rep.* 5:17740. doi: 10.1038/srep17740

Llano, D. A., Slater, B. J., Lesicko, A. M., and Stebbings, K. A. (2014). An auditory colliculothalamocortical brain slice preparation in mouse. *J. Neurophysiol.* 111, 197–207. doi: 10.1152/jn.00605.2013

Lucas, S. J., Michel, C. B., Marra, V., Smalley, J. L., Hennig, M. H., Graham, B. P., et al. (2018). Glucose and lactate as metabolic constraints on presynaptic transmission at an excitatory synapse. *J. Physiol.* 596, 1699–1721. doi: 10.1113/JP275107

Maranto, A. R. (1982). Neuronal mapping: a photooxidation reaction makes lucifer yellow useful for electron microscopy. *Science* 217, 953–955. doi: 10.1126/science.7112109

Marra, V., Burden, J. J., Crawford, F., and Staras, K. (2014). Ultrastructural readout of functional synaptic vesicle pools in hippocampal slices based on fm dye labeling and photoconversion. *Nat. Protoc.* 9, 1337–1347. doi: 10.1038/nprot.2014.088

Marra, V., Burden, J. J., Thorpe, J. R., Smith, I. T., Smith, S. L., Häusser, M., et al. (2012). A preferentially segregated recycling vesicle pool of limited size supports neurotransmission in native central synapses. *Neuron* 76, 579–589. doi: 10.1016/j.neuron.2012.08.042

Neher, E., and Sakaba, T. (2001). Combining deconvolution and noise analysis for the estimation of transmitter release rates at the calyx of held. *J. Neurosci.* 21, 444–461. doi: 10.1523/JNEUROSCI.21-02-00444.2001

Opazo, F., and Rizzoli, S. O. (2010). Studying synaptic vesicle pools using photoconversion of styryl dyes. *J. Vis. Exp.* e1790. doi: 10.3791/1790

Peddie, C. J., Domart, M.-C., Snetkov, X., O'Toole, P., Larijani, B., Way, M., et al. (2017). Correlative super-resolution fluorescence and electron microscopy using conventional fluorescent proteins in vacuo. *J. Struct. Biol.* 199, 120–131. doi: 10.1016/j.jsb.2017.05.013

Pulido, C., Trigo, F. F., Llano, I., and Marty, A. (2015). Vesicular release statistics and unitary postsynaptic current at single gabaergic synapses. *Neuron* 85, 159–172. doi: 10.1016/j.neuron.2014.12.006

Ratnayaka, A., Marra, V., Branco, T., and Staras, K. (2011). Extrasynaptic vesicle recycling in mature hippocampal neurons. *Nat. Commun.* 2:531. doi: 10.1038/ncomms1534

Ratnayaka, A., Marra, V., Bush, D., Burden, J. J., Branco, T., and Staras, K. (2012). Recruitment of resting vesicles into recycling pools supports nmda receptor-dependent synaptic potentiation in cultured hippocampal neurons. *J. Physiol.* 590(Pt 7), 1585–1597. doi: 10.1113/jphysiol.2011.226688

Rey, S. A., Smith, C. A., Fowler, M. W., Crawford, F., Burden, J. J., and Staras, K. (2015). Ultrastructural and functional fate of recycled vesicles in hippocampal synapses. *Nat. Commun.* 6:8043. doi: 10.1038/ncomms9043

Sabeva, N. S. and Bykhovskaia, M. (2017). Fm1-43 photoconversion and electron microscopy analysis at the drosophila neuromuscular junction. *Bio Protoc.* 7:e2523. doi: 10.21769/BioProtoc.2523

Shu, X., Lev-Ram, V., Deerinck, T. J., Qi, Y., Ramko, E. B., Davidson, M. W., et al. (2011). A genetically encoded tag for correlated light and electron microscopy of intact cells, tissues, and organisms. *PLoS Biol.* 9:e1001041. doi: 10.1371/journal.pbio.1001041

Smith, A. D., and Bolam, J. P. (1990). The neural network of the basal ganglia as revealed by the study of synaptic connections of identified neurones. *Trends Neurosci.* 13, 259–265. doi: 10.1016/0166-2236(90)90106-K

Viney, T. J., Lasztoczi, B., Katona, L., Crump, M. G., Tukker, J. J., Klausberger, T., et al. (2013). Network state-dependent inhibition of identified hippocampal ca3 axo-axonic cells *in vivo*. *Nat. Neurosci.* 16, 1802–1811. doi: 10.1038/nn.3550

Conflict of Interest Statement: The authors declare that the research was conducted in the absence of any commercial or financial relationships that could be construed as a potential conflict of interest.